

VALORIZATION AND CHARACTERIZATION OF WOOD OF THE JUJUBE SHELL: APPLICATION TO THE REMOVAL OF CATIONIC DYE FROM AQUEOUS SOLUTION

N. EL MESSAOUDI¹, M. EL KHOMRI¹, A. LACHERAI^{1*},
S. BENTAHAR¹, A. DBIK¹, B. BAKIZ²

¹Laboratory of Applied Chemistry and Environment, Department of Chemistry,
Faculty of Sciences, Ibn Zohr University, 80000, Agadir, Morocco

²Laboratory of Materials and Environment, Department of Chemistry,
Faculty of Sciences, Ibn Zohr University, 80000, Agadir, Morocco

*Corresponding author: a.lacherai@uiz.ac.ma

Abstract

In the present study, the powder of jujube shell (raw and modified) was tested for removing crystal violet (CV) from aqueous solution. The biosorbents were characterized by FTIR, SEM and pH_{ZPC} analysis. The biosorption behavior was studied in batch experiments such as biosorbent mass, contact time, temperature, initial dye pH, biosorbent particles size and initial dye concentration. The removal efficiency of crystal violet attained 95.84% and 98.16 %, using 0.2g of raw jujube shell (JS) and 0.1g of modified jujube shell with sodium hydroxide (NMJS), respectively. The obtained results indicate the endothermic nature of biosorption and that the biosorption system studied belongs to the second-order kinetic model. Equilibrium data of the biosorption process fitted very well to Langmuir model. The maximum biosorption monolayer capacities of crystal violet on raw and modified jujube shell were found to be 59.84 mg/g and 288.18 mg/g at 50°C, respectively. Thus, the raw jujube shell treatment with base is very effective and greatly improves the dye adsorption capacity.

Keywords: Jujube shell, Crystal violet, Biosorption, Isotherms, Kinetic.

1. Introduction

The issue of water, recurring problematic, is one of more strategic in our time and the most difficult because it is associated with life and she is not human product. Therefore, water pollution, accidentally or intentionally, becomes a universal scourge that causes environmental degradation, decreasing water quality and threatens public health. She is currently a major interest worldwide.

Nomenclatures

C_0	Initial dye concentration in the solution , mg/L
C_e	Concentration of solution at equilibrium, mg/L
K_1	Pseudo first-order rate constant of, 1/min
K_2	Pseudo second-order rate constant, g/mg/min
K_F	Freundlich constant ,(mg/g) (L/mg) ^{1/n}
K_L	Langmuir constant , L/mg
n	Adsorption intensity
q_e	Amount adsorbed of dye at equilibrium, mg/g
$q_{e,cal}$	Calculated equilibrium adsorption capacities , mg/g
$q_{e,exp}$	Experimental equilibrium adsorption capacities , mg/g
q_m	Maximum monolayer coverage capacity , mg/g
q_t	Amount adsorbed at time t, mg/g
r^2	Correlation coefficient
R_L	Dimensionless separation factor
S_p	Size of particles, μm
T	Temperature, K
t	Time , min
V	Volume of the solution , L
W	Weight of biosorbent , g

Greek Symbols

λ_{max}	Maximum absorption wavelength , nm
-----------------	------------------------------------

Abbreviations

ATR	Attenuated total reflectance
CV	Crystal Violet
FTIR	Fourier transform infrared
JS	Jujube shell
NMJS	NaOH-modified jujube shell
SEM	Scanning electron microscopy
UV	Ultraviolet
PZC	point of zero charge

The wastewater of textile industries is huge nuisance to the environment. In particular, the different dyes used cause serious problems because of their stability and their low biodegradability [1]. In addition they can cause water-borne diseases, some of which are considered carcinogenic and dangerous micro even when they exist in the form of traces [2].

To preserve water quality and protect the environment, it was necessary to implement pollution regulations. Discharge standards increasingly stringent were imposed. To meet these standards, it is important to implement efficient processes water treatment prior to discharge into the receiving environment.

Various processes have been used for the removal of dyes from industrial effluents, but remain the adsorption phenomenon commonly used because of its performance and its easy use [3].

In the various studies conducted by scientists, activated carbon is a good for treatment of discoloration but it poses problems of high cost it saturates quickly and it should be removed after use [4].The research then are directed to use lost cost adsorbents such as agricultural wastes, these latest very abundant in nature and effective to adsorb dyes from aqueous solutions.

The choice of jujube shell is dictated by the fact that it is abundant in several regions, cheap and especially for a valuation of said biomaterial. The *Ziziphus lotus* belongs to the family *Rhamnaceae* [5]. Its fruits used as edible food and traditional Chinese medicine [6], claimed to purify the blood and aid digestion [7].

The JS and NMJS were characterized with attenuated total reflectance-Fourier transform infrared (ATR-FTIR), scanning electron microscopy (SEM) analysis and pH point of zero charge (pH_{PZC}).The biosorption of crystal violet on JS and NMJS was carried out under various parameters such as biosorbent mass, contact time, initial dye pH, temperature, biosorbent particles size and initial dye concentration. Biosorption kinetic data of the biomass was tested by the pseudo first-order and the pseudo second-order kinetic models. The equilibrium sorption behavior of the biosorbent has been studied using the biosorption isotherm technique such as Langmuir and Freundlich models.

2. Materials and Methods

2.1. Preparation of biosorbents

The jujube core was collected in August 2014 near Tata, Morocco. It crushed to separate the seed and the shell. The jujube shell (Fig. 1) is washed and placed in an oven at 80 °C for 24 h, then ground in a grinder RETSCH SM100. The powder of jujube shell is sieved to different particles sizes such as 50-100, 100-315, 315-500 and 500-1000 μm . The NaOH-modified jujube shell (NMJS) is prepared by mixing 1g of jujube shell (JS) powder prepared with 100 mL of sodium hydroxide NaOH (0.1M), stirred for 24 h at room temperature. After decantation and filtration, the biomass washed with distilled water several times then dried in an oven at 80 °C for 24 h. The NMJS was crushed and sieved to the same of particles sizes of JS.



Fig. 1. Jujube shell used in this study.

2.2. Preparation of solutions dye

1gram of crystal violet dye (color index: 42555, chemical formula: $C_{25}H_{30}N_3Cl$, molecular weight: 407.99 g/mol) was dissolved in 1 liter of distilled water. Experimental dyeing solution of different concentrations was prepared by diluting the stock solution (1g/L). Chemical structure of CV is shown in Fig. 2.

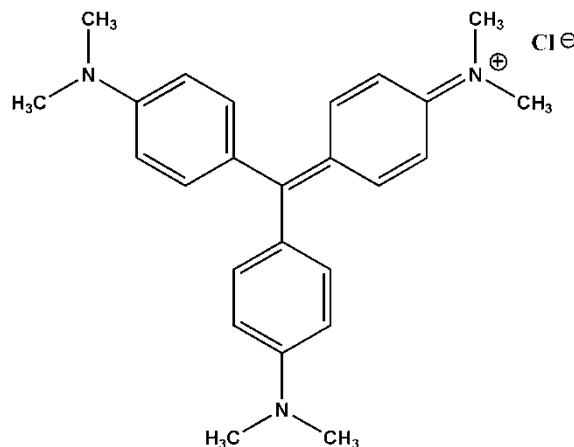


Fig. 2. Chemical structure of crystal violet dye.

2.3. Characterization of biosorbents

The surface functional groups and the structure were identified by ATR-FTIR spectroscopy. The FTIR spectra of JS and NMJS recorded with resolution 4 cm^{-1} in a JASCO4100 spectrometer, coupled to ATR technique. The morphology and structure of biosorbents surfaces are characterized using SEM on SUPRA 40 VP Colonne Gemini Zeiss instrument. The pH points of zero charge (pH_{PZC}) of JS and MNJS were determined using the following procedure: 50 mL of the NaCl solution (0.01 M) was placed in the flasks of 100mL. The initial pH (pH_i) of each solution was adjusted to values of 2 to 12 using HCl (0.01 M) or NaOH (0.01 M). An amount of 0.2 g of the biosorbent was added to each flask, and the final pH (pH_f) measured after 48 h of stirring at $25\text{ }^\circ\text{C}$. The value of pH_{PZC} is the point where the curve of ($pH_f - pH_i$) versus pH_i crosses the line equal to zero [8].

2.4. Batch experiments

Batch experiments were carried in an Erlenmeyer flasks by shaking a fixed mass JS (0.2 g) or NMJS (0.1g) with 50 mL diluted solution of dye at predetermined concentrations.

The flasks were agitated in a bath at a constant temperature by an external circulation thermostat. The effects of biosorbent mass (0.05, 0.1, 0.15, 0.2, 0.25 and 0.3 g), contact time (5, 10, 20, 30,40, 50, 60, 90, 120, 150 and 180 min), temperature (20, 30, 40 and $50\text{ }^\circ\text{C}$), biosorbent particles size (50-100 , 100-315, 315-500 and 500-1000 μm),pH (3, 4, 5, 6, 8, 9 and 10) and initial dye

concentration (100, 200, 300, 400, 500, 600, 700 and 800 mg/L) were evaluated during the present study.

The equilibrium concentrations of the solution were analyzed using a spectrophotometer (UV-Visible 2300-TECHCOMP). The standard calibration curve was prepared by recording the absorption of various concentrations values of crystal violet dye at a maximum absorption wavelength ($\lambda_{max} = 590$ nm).

Each experiment was carried out in duplicate and the average results are considered. The amount adsorbed at equilibrium q_e (mg/g) and the percentage removal of dye (%) on JS and NMJS were calculated using the following Eqns. (1) and (2), respectively.

$$q_e = \frac{(C_0 - C_e) \times V}{W} \tag{1}$$

$$\% \text{ Removal} = \frac{(C_0 - C_e) \times 100}{C_0} \tag{2}$$

where, C_0 (mg/L) and C_e (mg/L) are the initial and equilibrium concentrations of dye, respectively, V (L) is the volume of solution and W (g) is the weight of biosorbent used.

3. Results and Discussion

3.1. FTIR spectroscopy

The FTIR spectra of JS and NMJS are shown in Fig. 3. Comparing these spectra we can essentially note the appearance of a band at 1646 cm^{-1} attributed asymmetric axial of carboxylate ($-\text{COO}^-$) on spectrum of JS crude [9], formed according to the following reaction:

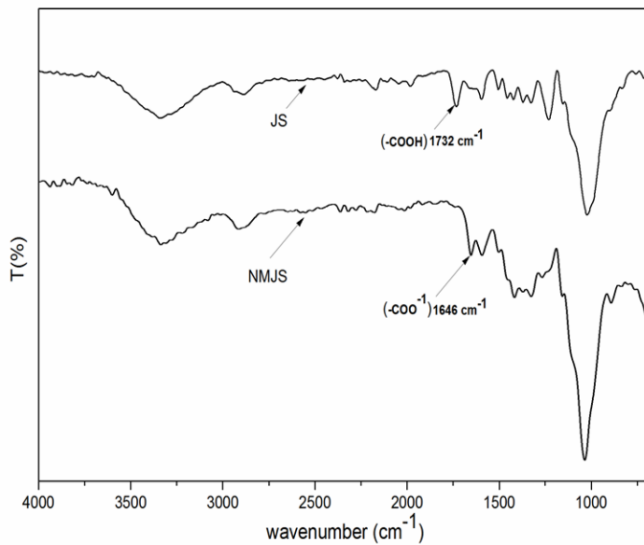
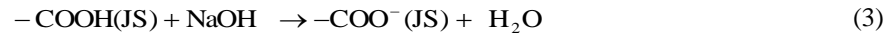


Fig. 3. FTIR spectra of JS and NMJS.

3.2. Scanning electron microscopy

Figure 4 shows the SEM images for the JS and NMJS. The JS micrograph, Figs. 4(a) and (b), shows that JS is formed of smooth grain with variable and random size and shape.

The NMJS micrograph, Fig. 4(c) confirms that the material is formed micron-size agglomerates with irregular cavities that could contribute to the biosorption of the dyes. This figure also proves that the structure has been modified NMJS upon treatment with NaOH.

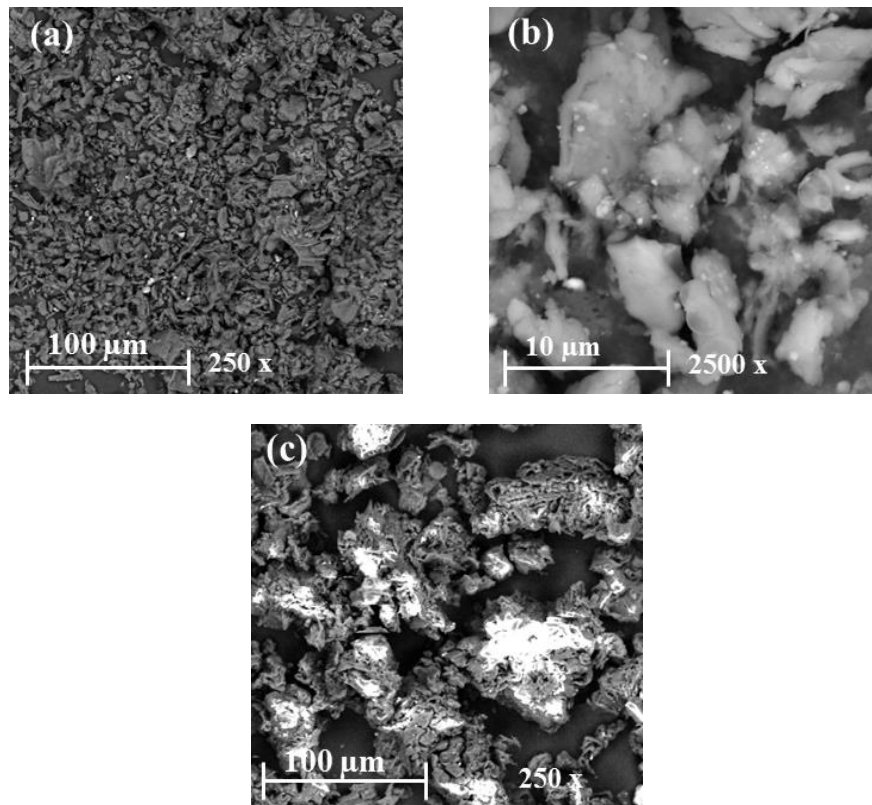


Fig. 4. SEM photographs: (a) JS ($\times 250$), (b) JS ($\times 2500$) and (c) NMJS ($\times 250$).

3.3. Effect of biosorbent mass

The amount of biosorbent presents a significant role in the biosorption process. The study of biosorbent mass for removal of crystal violet from aqueous solution was carried using masses of JS and NMJS biosorbents ranging from 0.05 to 0.3 g and fixing the in initial dye concentration, the contact time, the pH and volume of CV solutions at 100 mg/L, 60min, 5.46 and 50 mL, respectively. The results obtained are shown in Fig. 5.

The adsorption efficiency increased from 56.53% to 95.84% for JS and from 86.93% to 98.16% for NMJS as the adsorbent mass increased from 0.05 to 0.2 g and from 0.05 to 0.1 g of JS and NMJS, respectively.

The increase in the percentage dye removal with the adsorbent dose could be attributed to an increase in the adsorbent surface area, augmenting the number of adsorption sites available for adsorption [10]. After the 0.2 g of JS and 0.1 g of NMJS, the removal of CV is almost steady up the value 0.3 g. Indeed, any further addition of the adsorbent beyond this did not cause any significant change in the adsorption. This may be due to overlapping of adsorption sites as a result of overcrowding of adsorbent particles [11]. Therefore, in the following experiments, the biosorbent masses were fixed at 0.2 g for JS and 0.1 g for NMJS. We may also notice that the material treated with NaOH adsorbs better than crude.

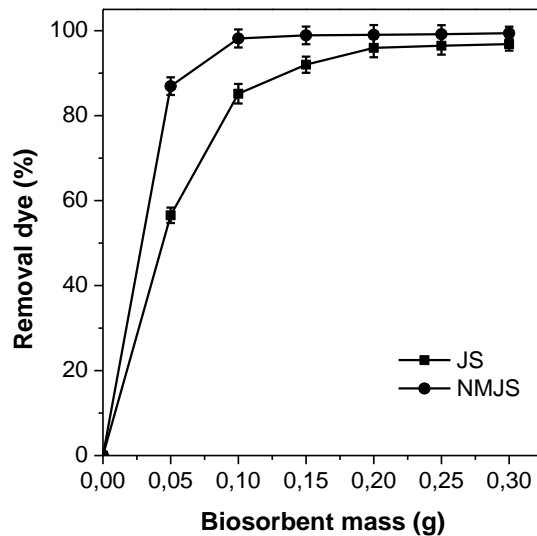


Fig. 5. Effect of biosorbent mass on the biosorption of CV on JS and NMJS:
 $C_0 = 100 \text{ mg/L}$, $t = 60 \text{ min}$, $T = 20 \text{ }^\circ\text{C}$, $pH = 5.46$, $S_p = 50\text{-}100 \text{ }\mu\text{m}$.

3.4. Effect of temperature

Temperature is amongst the most important parameters influencing the adsorption phenomenon. The temperature dependence of CV biosorption onto JS and NMJS was studied with a constant initial dye concentration of 100 mg/L at 60 min, 0.2 g of JS and 0.1 g of NMJS and $pH = 5.46$. We observed that the biosorption capacity increases with increasing in temperature as shown in Fig. 6, but this increase is very low. An increase in temperature also results in mobility of dye molecules [12]. Furthermore, when the temperature increases, it may produce swelling effect within the internal structure of JS and NMJS allowing to the dye molecule to penetrate more [13]. Therefore, the amount adsorbed of dye increases. This increase also indicates the endothermic nature of the dye biosorption onto JS and NMJS [14, 15].

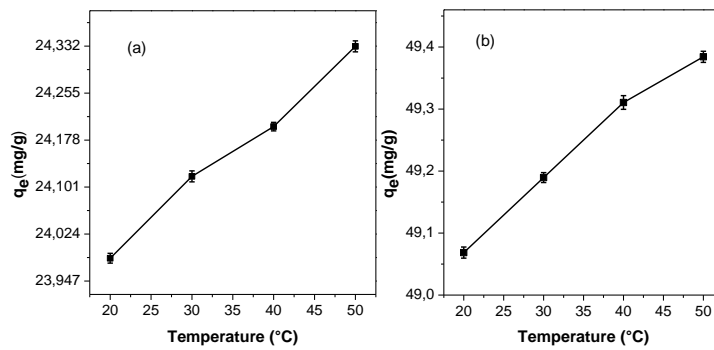


Fig. 6. Effect of temperature on the biosorption of CV on (a) JS and (b) NMJS: $C_0=100$ mg/L, 0.2 g of JS, 0.1 g of NMJS, $t=60$ min, $pH=5.46$, $S_p=50-100$ μm .

3.5. Effect of initial dye pH and pH_{PZC}

The pH value of initial solution is an important parameter in the biosorption process. Therefore, the biosorption of CV onto JS and NMJS was studied over a pH range of 3–10. The pH of dye solution was adjusted using the hydrochloric acid HCl (0.01 M) or NaOH (0.01 M). The results are shown in Fig. 7. The amount adsorbed of CV by JS and NMJS increases with the increasing in pH of the dye solution, appreciably up to $pH=6$. With further increase in pH from 6 to 10, the quantity adsorbed of CV increases, but this increase is low.

The increase in the amount adsorbed of CV on JS and NMJS, with increasing in pH of dye may be explained by the fact that the addition of cations H^+ to lower pH, results in the neutralization of the positive adsorbent load, therefore, the adsorption of CV decrease in very acidic environment. For against, when the pH increases there is a decrease of cations H^+ , so the biosorbent load is significantly negative which favors adsorption of CV [16]. Similar results were reported for biosorption of CV from aqueous solution onto coniferous pinus bark powder [17] and H_2SO_4 modified sugarcane bagasse [18].

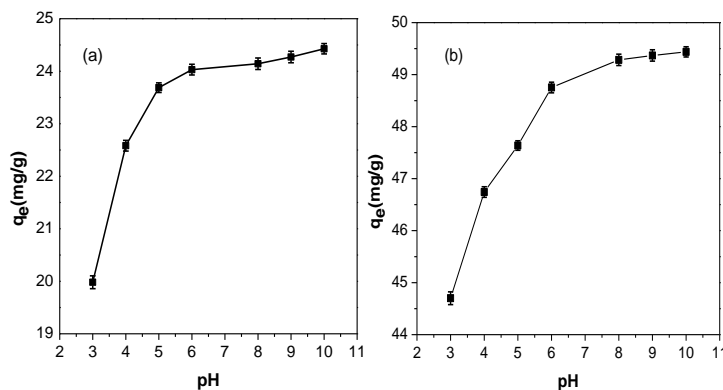


Fig. 7. Effect of initial dye pH on the biosorption of CV on (a) JS and (b) NMJS: $C_0=100$ mg/L, 0.2 g of JS, 0.1 g of NMJS, $T=20$ °C, $t=60$ min, $S_p=50-100$ μm .

From Fig. 8, the pH points of zero charge (pH_{PZC}) of JS and NMJS are found around 4.8 and 9.2, respectively. The pH_{PZC} of JS and NMJS have shown exhibits a negative charge at $pH > 4.8$ and $pH > 9.2$, and yields a positive charge at $pH < 4.8$ and $pH < 9.2$, respectively [19]. It is observed that the value of pH_{PZC} (NMJS) $> pH_{PZC}$ (JS), therefore, the NMJS is adsorb CV (basic dye) better than JS.

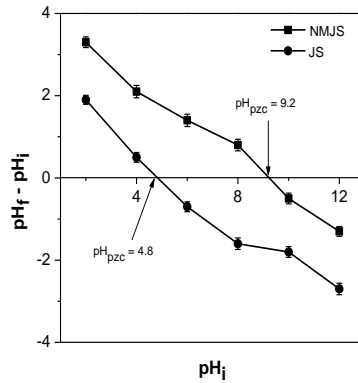


Fig. 8. Determination of pH points of zero charge of JS and NMJS.

3.6. Effect of biosorbent particles size

The biosorption of CV dye was studied at for different particles size (50-100, 100-315, 315-500 and 500-1000 μm) of the JS and NMJS biosorbents in optimal conditions. Figure 9 shows that amounts adsorbed of CV by JS and NMJS increases from 4.31 to 23.85 mg/g and from 10.21 to 49.04 mg/g, respectively, when biosorbent particles size decreases from 500-1000 to 50-100 μm . This increase of amounts adsorbed due to the increase in the surface area and accessibility of the biosorbent pores for the dye.

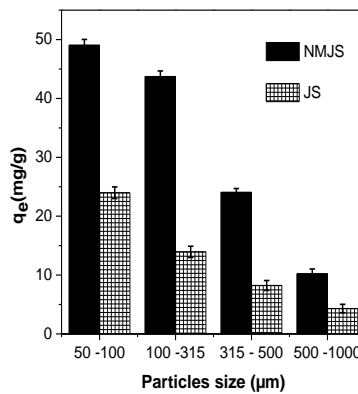


Fig. 9. Effect of JS and NMJS particles size on the biosorption of CV: $C_0 = 100$ mg/L, 0.2 g of JS, 0.1 g of NMJS, $T = 20$ °C, $t = 60$ min, $pH = 5.46$.

3.7. Effect of contact time

The contact time between the biosorbent and adsorbate has of significant importance for the designing of biosorption system and its scale application. The effect of contact time on removal of CV by JS and NMJS was performed by batch experiments to reach equilibrium, as indicated in Fig. 10.

The results indicate that during the biosorption process, initially a fast dye uptake by the biosorbent was observed which was followed by the slower dye removal. This can be explained by the fact that initially all the active sites on the surface of biosorbents are vacant and dye molecules easily occupy these binding sites. With the progress of reaction, the binding sites become saturated and biosorption process becomes slower to reach equilibrium after the occupation of the majority of sites by CV [20].

The equilibrium time for raw and treated biomass was found to be 60 min. After this time duration, no significant change in the biosorption capacity of wood of the jujube shell was observed. In the following work a contact time of 60 minutes seems more than enough to reach equilibrium.

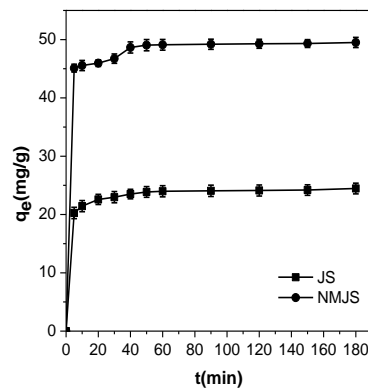


Fig. 10. Effect of contact time on the biosorption of CV onto JS and NMJS: $C_0=100$ mg/L, 0.2g of JS, 0.1 g of NMJS, $pH=5.46$, $T= 20$ °C, $S_p=50-100$ μ m.

3.8. Kinetic biosorption

A quantitative understanding of the adsorption is possible using kinetic models. Kinetic of pseudo-first-order model can be written as follows [21]:

$$\text{Log} (q_e - q_t) = \text{Log} (q_e) - \frac{K_1}{2.303} t \quad (4)$$

Where, q_t (mg/g) and q_e (mg/g) are the amounts adsorbed at time t and equilibrium, respectively and K_1 (1/min) is the pseudo-first-order rate constant.

The results are shown in Fig. 11. The constant K_1 , the amount adsorbed calculated $q_{e,cal}$ and the correlation coefficient r^2 are given in Table 1. The calculation shows that $q_{e,cal}$ dye is rather low compared with the experimental quantities $q_{e,exp}$. This observation leads us to say that the biosorption of CV onto

JS and NMJS not express a controlled diffusion process since it does not follow the equation of pseudo-first order.

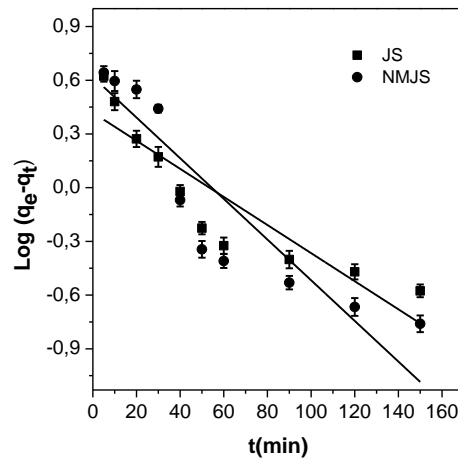


Fig. 11. Pseudo first-order model kinetic of biosorption of CV on JS and NMJS: $C_0=100$ mg/L, 0.2g of JS, 0.1 g of NMJS, $T=20$ °C, $pH=5.46, S_p=50-100$ μ m.

The equation of the pseudo second-order model can be expressed as follows [22]:

$$\frac{t}{q_t} = \frac{1}{K_2 q_e^2} + \frac{1}{q_e} t \tag{5}$$

where, K_2 (g/mg/min) is the pseudo second-order rate constant.

Figure 12 shows the application of the pseudo-second order kinetic model to the results obtained for the biosorption of CV onto JS and NMJS. The $q_{e,cal}$, the constant K_2 and the correlation coefficient r^2 are given in Table 1.

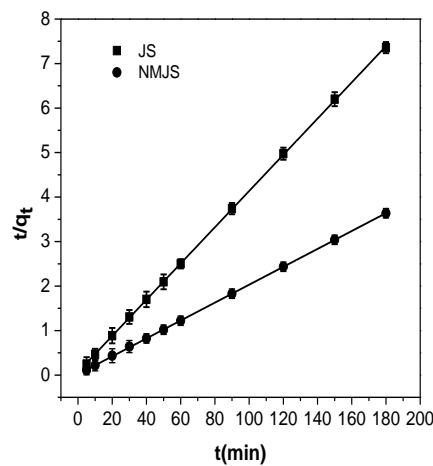


Fig. 12. Pseudo second-order kinetic model of biosorption of CV on JS and NMJS: $C_0=100$ mg/L, 0.2g of JS, 0.1 g of NMJS, $T=20$ °C, $pH=5.46, S_p=50-100$ μ m.

The quantities calculated $q_{e,cal}$ very close to the experimental values $q_{e,exp}$. This result indicates that the biosorption systems studied belongs to the pseudo second-order kinetic model.

Table 1. Kinetic models parameters for CV biosorption.

Biosorbent	Pseudo first-order model			
	$q_{e,exp}$ (mg/g)	$q_{e,cal}$ (mg/g)	K_1 (1/min)	r^2
JS	24.46	2.53	0.018	0.799
NMJS	49.50	3.53	0.024	0.798
Biosorbent	Pseudo first-order model			
	$q_{e,exp}$ (mg/g)	$q_{e,cal}$ (mg/g)	K_2 (g/mg/min)	r^2
JS	24.46	24.55	0.025	0.999
NMJS	49.50	49.75	0.018	0.999

3.9. Biosorption isotherms

It is important to study equilibrium isotherm for the design of the biosorption system. Two models biosorption isotherms, Langmuir and Freundlich are have been designed in the range 100-800 mg/L, keeping parameters fixed at 0.2 g for JS, 0.1 g for NMJS, 60 min, 50°C and pH=5.46. Figure 13 shows the transformed linear equations corresponding to these two isotherms. The Langmuir equation can be described by the following linear form [23]:

$$\frac{C_e}{q_e} = \frac{1}{q_m K_L} + \frac{C_e}{q_m} \quad (6)$$

where, K_L (L/mg) is the Langmuir constant and q_m (mg/g) is the maximum amount of adsorbate retained on the medium used.

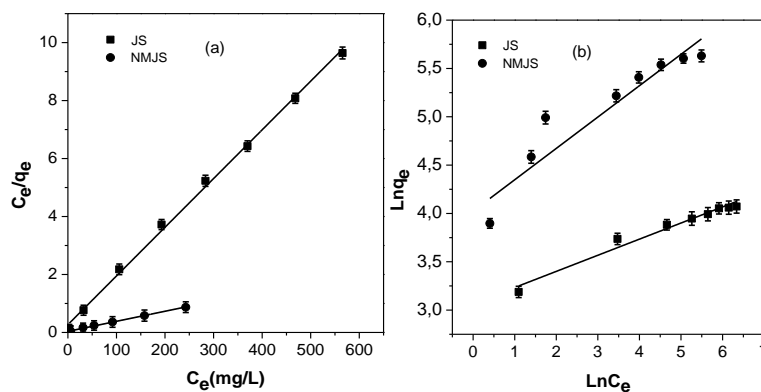


Fig. 13. (a) Langmuir and (b) Freundlich isotherms for biosorption of CV on JS and NMJS: $C_0=100-800$ mg/L, 0.2 g of JS, 0.1 g of NMJS, $t=60$ min, $T=50^\circ\text{C}$, $\text{pH}=5.46$, $S_p=50-100$ μm .

Isotherm Langmuir has several advantages, K_L value is related to the strength of interaction between the adsorbed molecule and the solid surface and q_m value expresses the amount of solute, its simplicity, the fact that the parameters K_L and q_m have physical significance is attached quoted per gram of solid, the surface is

considered totally covered by a single molecular layer. The essential characteristics of the Langmuir isotherm can be expressed in terms of a dimensionless separation factor R_L , which is defined by [24]:

$$R_L = \frac{1}{1 + K_L C_0} \tag{7}$$

The R_L value indicates the mode sorption isotherm process, if the process is unfavorable ($R_L > 1$) or linear ($R_L = 1$) or favorable ($0 < R_L < 1$) or irreversible ($R_L = 0$). The linearized Freundlich equation is represented by the following equation [25]:

$$\ln(q_e) = \ln(K_F) + \frac{1}{n} \ln(C_e) \tag{8}$$

where, K_F ((mg/g) (L/mg)^{1/n}) is the Freundlich constant and n is the intensity of the adsorption.

The characteristics parameters of each model are listed in Table 2.

Table 2. Isotherm parameters for CV biosorption.

Biosorbent	Langmuir			
	K_L (L/mg)	q_m (mg/g)	R_L	r^2
JS	0.055	59.84	0.021- 0.152	0.998
NMJS	0.094	288.18	0.013- 0.095	0.997
	Freundlich			r^2
	K_F ((mg/g) (L/mg) ^{1/n})	$1/n$		
JS	21.56		0.165	0.967
NMJS	61.02		0.306	0.874

The high values of r^2 demonstrated that the Langmuir model was the more to the represent the biosorption of CV on JS and NMJS. Based on the Langmuir isotherm, the maximum monolayer biosorption capacities obtained CV on JS and NMJS were 59.84 mg/g and 288.18 mg/g of CV at 50°C, respectively.

Table 3 depicts the values of maximum biosorption capacities of various plant-origin biosorbents used for the removal of crystal violet. We note the NMJS is good biosorbent compared with other examples.

Table 3. Comparison of maximum biosorption capacities of some biosorbents for removal of CV.

Biosorbent	q_m (mg/g)	Reference
Calotropisprocera	4.14	[26]
Jackfruit leaf powder	43.39	[27]
Ceriporia lacerates P2	239.25	[28]
Formosa papaya seed powder	85.99	[29]
Peel of Cucumis sativa	34.24	[30]
Skin almonds waste	85.47	[31]
Tomato plant root	94.33	[32]
Treated ginger waste	277.7	[33]
Jujube shell	59.84	This study
NaOH-modified jujube shell	288.18	This study

4. Conclusion

In this study the removal of basic dye from aqueous solution using a vegetable origin and low-cost material, such as wood of the jujube shells (raw or modified with NaOH), was investigated involving crystal violet as a pollutant model.

The biosorption of CV onto JS and NMJS increased with increasing in temperature, contact time, initial dye pH, biosorbent particles size, initial dye concentration and biosorbent mass.

The results of FTIR indicate the presence of $-\text{COO}^-$ groups on the surface of NMJS responsible for increases the biosorption capacity of CV. SEM analysis shows the increase in porosity of the JS after treatment with NaOH.

The biosorption of CV on JS and NMJS was according to the Langmuir second order-model kinetic models. The maximum monolayer biosorption capacities of crystal violet onto the JS and NMJS were 59.84 mg/g and 288.18 mg/g at 50 °C, respectively.

Finally, the jujube shell, especially modified with sodium hydroxide, may be an effective and alternative adsorbent for removing dyes from aqueous solution in industrial processes.

References

1. Mehrorang, G.; Shaaker H.; Behnaz B.; Farahnaz K.; and Gholamreza, G. (2013). *Saccharomyces cerevisiae* for the biosorption of basic dyes from binary component systems and the high order derivative spectrophotometric method for simultaneous analysis of brilliant green and methylene blue. *Journal of Industrial and Engineering Chemistry*, 19 (1), 227-233.
2. De Lima, R.O.A.; Bazo, A.P.; Salvadori, D.M.F.; Rech, C.M.; Oliveira, D.P.; and Umbuzeiro, G.A.(2007). Mutagenic and carcinogenic potential of a textile azo dye processing plant effluent that impacts a drinking water source. *Mutation Research*, 626, 53-60.
3. Ali, I.; and Gupta, V.K. (2006). Advances in water treatment by adsorption technology. *Nature Protocol*, 1(6), 2661-2667.
4. Hameed, B.H.; and El-Khaiary, M.I. (2008). Removal of basic dye from aqueous medium using a novel agricultural waste material: Pumpkin seed hull. *Journal of Hazardous Materials*, 155(3), 601-609.
5. Maraghni, M.; Gorai, M.; and Neffati, M. (2010). Seed germination at different temperatures and water stress levels, and seedling emergence from different depths of *Ziziphus lotus*. *South African Journal of Botany*, 76(3), 453-459.
6. Adeli, M.; and Samavati, V.(2015). Studies on the steady shear flow behavior and chemical properties of water soluble polysaccharide from *Ziziphus*. *International Journal of Biological Macromolecules*, 72,580 -587.
7. Tripathi, M.; Pandey, M.B.; Jha, R.N.; Pandey, V.B.; Tripathi, P.N.; and Singh, J. (2001). Cyclopeptide alkaloids from *Ziziphus jujuba*. *Fitoterapia*, 72(5), 507-510.

8. Ofomaja, A.E.; and Ho, Y.S. (2007).Effect of pH on cadmium biosorption by coconut copra meal. *Journal of Hazardous Materials*, 139, 356 -362.
9. Karla, A.G.G.; Leandro, V.A.G.; Tânia, M.S.M.; and Laurent, F.G. (2013). Adsorption studies of methylene blue and gentian violet on sugarcane bagasse modified with EDTA dianhydride (EDTAD) in aqueous solutions: kinetic and equilibrium aspects. *Journal of Environmental Management*, 118, 135-143.
10. Saeeda, A.; Sharif, M.; and Iqbal, M. (2010).Application potential of grapefruit peel as dye sorbent: Kinetics, equilibrium and mechanism of crystal violet adsorption. *Journal of Hazardous Materials*, 179(1-3), 564-572.
11. Senthil, K. P.; and Kirthika, K. (2009). Equilibrium and kinetic study of adsorption of nickel from aqueous solution onto bael tree leaf powder. *Journal of Engineering Science and Technology*, 4, 351-363.
12. Alkan, M.; and Doğan, M.(2003).Adsorption kinetics of victoria blue onto perlite. *Fresenius Environmental Bulletin*, 12 (5), 418-425.
13. Asfour, H.M.; Fadali, O.A.; Nassar, M.M.; and El-Geundi, M.S. (1985). Equilibrium studies on adsorption of basic dyes on hardwood, *Journal of Chemical Technology and Biotechnology*, 35 (1), 21-27.
14. Mittal, A.; Mittal, J.; Malviya, A., Kaur, D.; and Gupta, V. K. (2010). Adsorption of hazardous dye crystal violet from waste water by waste materials. *Journal of Colloid and Interface Science*, 343(2), 463-473.
15. Ncibi, M.C.; Borhane, M.; and Mongi, S. (2006). Studies on the biosorption of textile dyes from aqueous solutions using posidonia oceanica (L.) leaf sheath fibers. *Adsorption Science and Technology*, 24(6), 461-473.
16. Chaker, N.M.; Mahjoub, B.; and Seffen, M. (2007). Kinetic and equilibrium studies of methylene blue biosorption by posidonia oceanica (L.) fibres. *Journal of Hazardous Materials*, 139(2), 280-285.
17. Rais, A. (2009). Studies on adsorption of crystal violet dye from aqueous solution onto coniferous pinus bark powder (CPBP). *Journal of Hazardous Materials*, 171(1-3), 767-773.
18. Chakraborty, S.; Chowdhury, S.; and Papita, D.S.(2012). Batch removal of crystal violet from aqueous solution by H₂SO₄ modified sugarcane bagasse: Equilibrium, kinetic, and thermodynamic profile. *Separation Science and Technology*, 47, 1898-1905.
19. Singh, J.; Ali, A.; Jaswal, V.S.; and Prakash, V. (2014). Desalination of Cd²⁺ and Pb²⁺ from paint industrial wastewater by aspergillusniger decomposed citrus limetta peel powder. *International Journal of Environmental Science and Technology*, 12(8), 2523-2532.
20. El-Sayed, G.O. (2011). Removal of methylene blue and crystal violet from aqueous solutions by palm kernel fiber. *Desalination*, 272(1-3), 225-232.
21. Bouhamed, F.; Elouear, Z.; and Bouzid, J. (2012). Adsorptive removal of copper (II) from aqueous solutions on activated carbon prepared from Tunisian date stones: Equilibrium, kinetics and thermodynamics. *Journal of the Taiwan Institute of Chemical Engineers*, 43(5), 741-749.
22. Chiou, M.S.; and Li, H.Y. (2002). Equilibrium and kinetic modeling of adsorption of reactive dye on cross-linked chitosan beads. *Journal of Hazardous Materials*, 93(2), 233-248.

23. Langmuir, I. (1918). The adsorption of gases on plane surfaces of glass, mica and platinum. *Journal of the American Chemical Society*, 40(9), 1361-1403.
24. Anjali, P.; Satyajit, P.; and Sandip, S.(2013). Synergistically improved adsorption of anionic surfactant and crystal violet on chitosan hydrogel Beads. *Chemical Engineering Journal*, 217, 426-434.
25. Freundlich, H.M.F. (1906). Over the adsorption in solution. *Journal of Physical Chemistry*, 57, 385-470.
26. Ali, H.; and Muhammad, S.K. (2008). Biosorption of crystal violet from water on leaf biomass of calotropisprocera. *Journal of Environmental Science and Technology*, 1(3), 143-150.
27. Saha, P.D.; Chakraborty, S.; and Chowdhury, S. (2012). Batch and continuous (fixed-bed column) biosorption of crystal violet by *Artocarpusheterophyllus* (jackfruit) leaf powder. *Colloids and Surfaces B: Biointerfaces*, 92,262- 270.
28. Yonghui, L.; Xingbing, H.; Guomin H.; Qijian, T.; and Wenyong, H. (2012). Removal of crystal violet from aqueous solution using powdered mycelia biomass of *ceriporia lacerates* P2. *Journal of Environmental Sciences*, 23(12), 2055-2062.
29. Pavan, F.A.; Camacho, E.S.; Lima, E.C.; Dotto, G.L.; Branco, V.T.A.; and Dias, S.L.P.(2014). Formosa papaya seed powder (FPSP): Preparation, characterization and application as an alternative adsorbent for the removal of crystal violet from aqueous phase. *Journal of Environmental Chemical Engineering*, 2(1), 230-238.
30. Smitha, T.;Thirumalisamy, S.; and Manonmani, S. (2012). Equilibrium and kinetics study of adsorption of crystal violet onto the peel of *cucumis sativa* fruit from aqueous solution. *E-Journal of Chemistry*, 9 (3), 1091-1101.
31. Atmani, F.; Bensmaili, A.; and Mezenner, N.Y. (2009). Synthetic textile effluent removal by skins almonds waste. *Journal of Environmental Science and Technology*, 2(4), 153-169.
32. Chellapandian, K.; Natesan B.; and Thayumanavan, P. (2009). Removal of plant poisoning dyes by adsorption on tomato plant root and green carbon from aqueous solution and its recovery. *Desalination*, 249(3), 1132-1138.
33. Rajeev, K.; and Rais, A. (2011). Biosorption of hazardous crystal violet dye from aqueous solution onto treated ginger waste (TGW). *Desalination*, 265(1-3), 112-118.